

Polymeric Composite Materials Based on Silicate: I-Synthesis, Characterization and Formation Mechanism

Abou Mesalam MM¹, Abass MR^{1*}, Ibrahim AB¹, Zakaria ES¹ and Hassan AM²

¹Atomic Energy Authority, Hot Labs Centre, P. Code 13759, Cairo, Egypt

²Faculty of Science, Al-Azhar University, Cairo, Egypt

*Corresponding author: MR Abass, Atomic Energy Authority, Hot Labs Centre, P. Code 13759, Cairo, Egypt, Tel:

+20 102 722 7142; E-mail: mohamed.ragab@eaea.org.eg; mohamed.ragab2014300@yahoo.com

Received: December 03, 2017 Accepted: December 27, 2017; Published: December 28, 2017

Abstract

Magneso-silicate has been synthesized by precipitation technique. Polyacrylamide acrylic acid and polyacrylamide acrylonitrile impregnated with inorganic silicate, have been synthesized by subjected co-monomers to gamma radiation initiated polymerization at radiation doses 25, 65 and 90 KGy. The structure for these composites was investigated by sequential x-ray fluorescence spectrometer, x-ray diffraction, differential thermal- thermogravimetric analyses and infrared spectroscopy. The impregnation of magneso-silicate into the polymeric composites was carried out by condensation polymerization.

Keywords: *Magneso-silicate; Co-monomers; Gamma radiation; Condensation polymerization.*

Introduction

Inorganic ion exchange materials play an important role in analytical chemistry, based originally on their resistance to chemical attack as well as their thermal and radiation resistance [1,2]. Polymers can be synthesized through various techniques such as radical, cationic and anionic polymerization [3]. The structural, mechanical and thermal properties can be investigated through different kinds of characterization methods to determination of structure property relationships [3,4]. Recently, polymers have been applied in various fields such as automotive, construction, electronic, cosmetic and pharmaceutical industries due to its advantageous material properties. Functional polymers of photochromic [5], electrochromic [6] and optoelectronic [7] functions were developed recently. The use of polymers with tunable refractive properties as optical modulators, optical filters, or electro optic waveguide devices has been reported [8]. The development of new inorganic ion exchangers with characteristic

properties is still need attention and their utility in diverse fields is yet to be explored. Synthetic ion exchangers are used on a wide range for different applications, ranging from environmental remediation [1,9,10], water softening [10], hydrometallurgy [10] and selective adsorption [11,12] to medical applications [13-15]. Different materials based on silicate salts and poly acrylamide acrylic acid silicon titanate were synthesized earlier [1,11,16] and used for removal of some heavy metals from industrial and hazardous waste solutions.

In this work magnesio-silicate (MgSi) as inorganic ion exchange material was synthesized using precipitation technique. Polyacrylamide acrylic acid P (AM-AA), polyacrylamide acrylonitrile P (AM-AN), polyacrylamide acrylic acid magnesio-silicate {P (AM-AA)-MgSi} and polyacrylamide acrylonitrile magnesio-silicate {P (AM-AN)-MgSi} composites have been synthesized by gamma radiation initiated polymerization at radiation doses 25, 65 and 90 KGy. The prepared composite materials were analyzed by different analytical techniques and a new ion exchange character was represented compared to the original ones.

Experimental Procedure

All chemicals and reagents used were of analytical grade.

Synthesis of magnesio-silicate composite

Magnesio-silicate ion exchange material was synthesized as reported earlier [1,11,14] by the addition of equimolar solutions (0.5 M) of magnesium chloride to sodium metasilicate dropwisely with volumetric ratio for (Mg/Si) equal 1.5 with continuous stirring in a water bath adjusted at $60 \pm 1^\circ\text{C}$. The mixed solutions were immediately hydrolyzed in demineralized water. Diluted ammonia solution was added to the mixture until complete precipitation attained. The precipitate formed was kept in the mother solution to overnight standing. The precipitate was washed several times with distilled water, and then washed by 0.1 M HNO_3 to remove impurities and Cl^- ions. The precipitate re-washed by distilled water to remove NO_3^- ions. After drying at $60 \pm 1^\circ\text{C}$, solid was poured in near boiling distilled water heated at $70 \pm 1^\circ\text{C}$ to break the solid and remove air trapped inside the solid, then re-dried at $60 \pm 1^\circ\text{C}$. The obtained solid was ground and store at room temperature.

Synthesis of monomer solutions

The investigated monomer solutions, acrylamide (AM), acrylic acid (AA) and acrylonitrile (AN) were prepared by dissolving 10% of each monomer in deoxygenated water.

Synthesis of co-monomer solutions

The acrylamide (AM) monomer solution was mixed with an aqueous solutions of acrylic acid (AA) and acrylonitrile (AN) by drop with addition at constant stirring and room temperature with volumetric ratio equal unity for the preparation of (AM+AA) and (AM+AN) co-monomers, respectively. Then the (AM+AA) and (AM+AN) co-monomers were mixed with equimolar solutions (0.5M) of sodium metasilicate and magnesium chloride

hexahydrate by drop with addition at constant stirring and room temperature with volumetric ratio (AM-AA-Mg-Si) and (AM-AN-Mg-Si) equal 1:1:1.5:1, respectively.

Synthesis of P (AM-AA), P (AM-AN), {P (AM-AA)-MgSi} and {P (AM-AN)-MgSi} composites

P (AM-AA), P (AM-AN), {P (AM-AA)-MgSi} and {P (AM-AN)-MgSi} composites were prepared by subjected mixtures of (AM+AA), (AM+AN), (AM+AA+Mg+Si) and (AM+AN+Mg+Si) co-monomers to gamma radiation at radiation doses 25, 65 and 90 KGy with dose rate 1.05 KGy/h. After irradiation, the obtained hydrogel was cut into small pieces with a stainless steel scissors, soaked in acetone for removal of unreacted monomers, washed with water [17], dried at 50°C, grained, sieved for different mesh sizes and stored at room temperature [18].

Composition and characterization of synthesized composites

IR spectra of MgSi, P (AM-AA), P (AM-AN), {P (AM-AA)-MgSi} and {P (AM-AN)-MgSi} composites prepared at different radiation doses were carried out by mixing of the solid with KOH in ratio 1:5 and ground to a very fine powder. A transparent disc was formed in a moisture free atmosphere. The IR spectra were recorded using BOMEM FTIR spectrometer in the range 400–4000 cm^{-1} .

The stoichiometry of the constituents in MgSi and polymeric composites based to silicate prepared at different radiation doses were determined using Philips sequential x-ray spectrometer-2400. The solid samples were ground to very fine powders and then mixed with H₃BO₃ as a binder to facilitate the pressing process. The mixture was pressed in a sample holder of 40 mm diameter aluminum cups and pressed on pressing machine at 20 psi to produce a sample with the diameter of 40 mm and 5 mm thickness. The concentrations of magnesium and silicone were measured according to Super-Q quantitative application program.

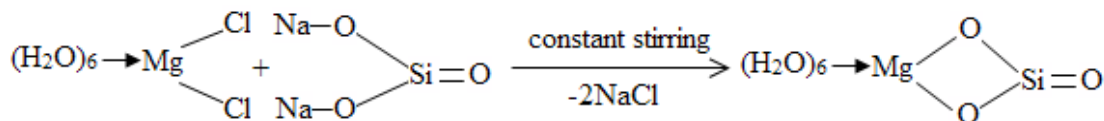
X-ray diffraction patterns of prepared composites were carried out using a Shimadzu XD-D1, X-ray diffractometer with Cu-K α radiation tube source ($\lambda=1.5406\text{\AA}$) and graphite monochromator operating at 30 kV and 30 mA. The measurements were done in 2 θ ranges from 4 to 90 with scan speed 2°/min.

Prepared composites (20 mg) were analyzed for DTA and TGA with sample holder made of Pt in N₂ atmosphere using a Shimadzu DTG-60H. The heating rate was maintained at 10°C/min with using alumina powder as reference material.

Results and Discussion

The scope of this study is the attempt to synthesize a high chemical stable inorganic, organic and composite ion exchange materials with high selectivity for some heavy metals. MgSi, P (AM-AA), P (AM-AN), {P (AM-AA)-MgSi} and {P (AM-AN)-MgSi} composites prepared at different radiation doses have been synthesized with complete characterization for ion exchange materials.

Magneso-silicate (MgSi) was prepared earlier in our laboratories [11]. The formation mechanism of prepared MgSi can be represented as shown in SCHEME 1. Magneso-silicate material was obtained by substitution of two Na⁺ ions by one Mg²⁺ ion and elimination of two molecules of NaCl.

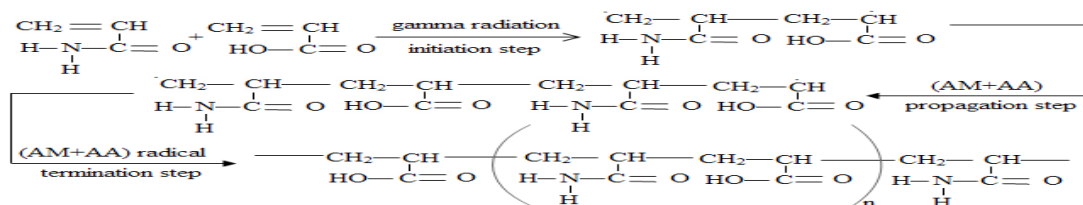


SCHEME 1. Formation mechanism of magneso-silicate composite.

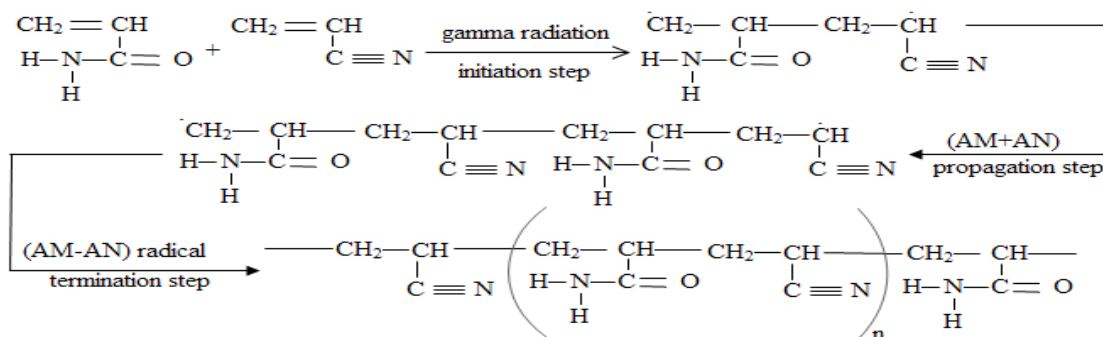
P (AM-AA), P (AM-AN), {P (AM-AA)-MgSi} and {P (AM-AN)-MgSi} composites were prepared as mentioned before in the experimental part by gamma radiation initiated co-polymerization of (AM+AA), (AM+AN), (AM+AA+Mg+Si) and (AM+AN+Mg+Si) co-monomers at radiation doses 25, 65 and 90 KGy. In gamma radiation initiated, the co-polymerization polymer complexes were formed which may be attributed to the possible steps [19]: preparation of the polymer by the generated radicals from the co-monomers, and the propagation of the co-monomer associated with the polymer by free radicals generated in the system [16,20].

The formation mechanism of P (AM-AA) copolymers can be represented as shown in SCHEME 2, when (AM+AA) co-monomer subjected to gamma radiation, breaking down was carried out for double bond of (AM) and (AA) to form covalent bond between C atoms of (AM) and (AA), the polymerization in the chain occurred by addition polymerization [21]. (AM+AA) free radical was obtained. (AM+AA) free radical react with (AM+AA) co-monomer to form chain propagation. Finally, the chains were coupled with another (AM-AA) free radicals to obtain P (AM-AA) copolymer.

The formation mechanism of P (AM-AN) copolymers can be shown in SCHEME 3, from this scheme; when (AM+AN) co-monomer subjected to gamma radiation, breaking down was carried out for double bond of (AM), (AN) to form covalent bond between C atoms of (AM) and (AN), the polymerization in the chain occurred by addition polymerization [21]. (AM+AN) free radical was obtained. (AM+AN) free radical react with (AM-AN) co-monomer to form chain propagation. Finally, the chains were coupled with another (AM-AN) free radicals to obtain P (AM-AN) copolymer.



SCHEME 2. Formation mechanism of polyacrylamide acrylic acid copolymer.

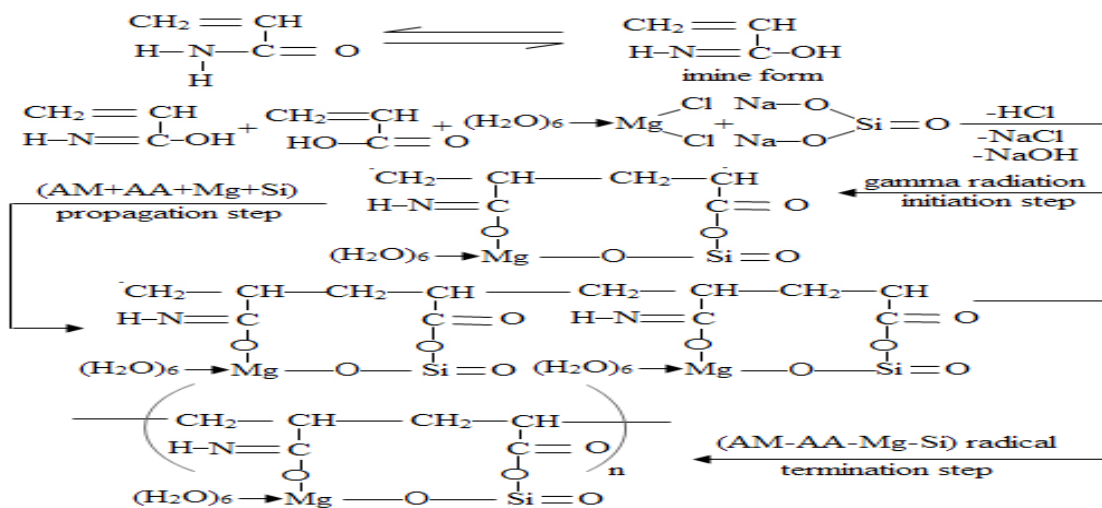


SCHEME 3. Formation mechanism of polyacrylamide acrylonitrile copolymer.

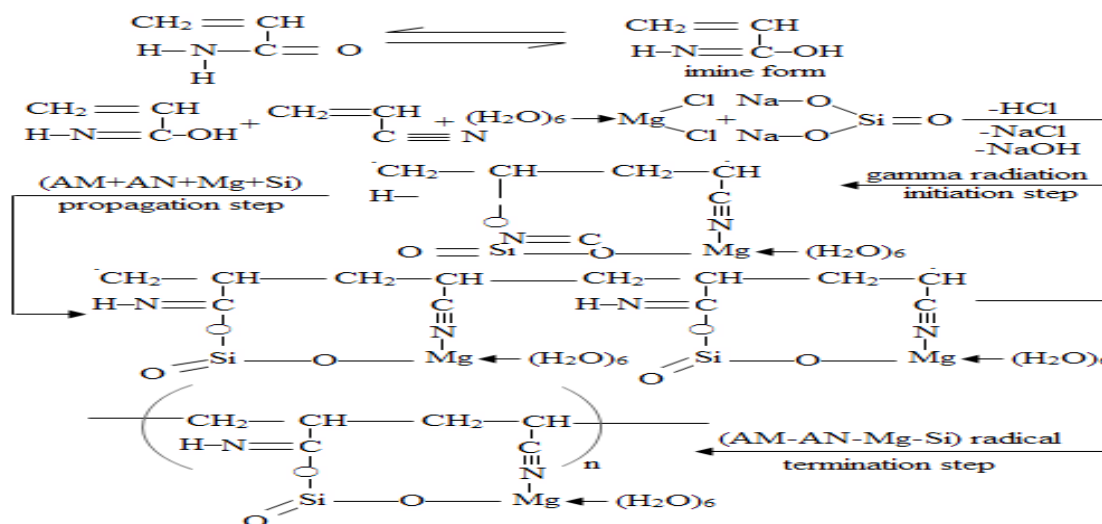
The formation mechanism of {P (AM-AA)-MgSi} composite can be represented as shown in SCHEME 4, the reaction started by converting of (AM) monomer to imine form in solution. Then imine form react with (AA+Mg+Si) to form (AM-AA-Mg-Si) co-monomer, and subjected to gamma radiation, breaking down was carried out for double bond of (AM) and (AA) and formation of covalent bond between C atoms of (AM) and (AA), the polymerization in the chain between (AM) and (AA) occurred by addition polymerization, where polymerization of (Mg-Si) in the chain was occurred by condensation polymerization [21] by elimination of OH^- of carboxylate group of (AA) with Na^+ of Na_2SiO_3 to form ionic bond between O atom of carboxylate group and Si atom of Na_2SiO_3 and elimination of H^+ of imine form with Cl^- of $\text{MgCl}_2 \cdot 6\text{H}_2\text{O}$ to form ionic bond between O atom of imine form and Mg atom of $\text{MgCl}_2 \cdot 6\text{H}_2\text{O}$ and elimination Na^+ of Na_2SiO_3 with Cl^- of $\text{MgCl}_2 \cdot 6\text{H}_2\text{O}$ to form ionic bond between O atom of Na_2SiO_3 and Mg atom of $\text{MgCl}_2 \cdot 6\text{H}_2\text{O}$ to form (AM-AA-Mg-Si) free radicals. (AM-AA-Mg-Si) free radical react with (AM-AA-Mg-Si) co-monomer to form chain propagation. Finally, the chains were coupled with another (AM-AA-Mg-Si) free radical to obtain {P (AM-AA)-MgSi} composite.

The formation mechanism of {P (AM-AN)-MgSi} composite was shown in SCHEME 5, the reaction started by converting of (AM) monomer to imine form in solution. Then imine form reacted with (AN+Mg+Si) to form (AM-AN-Mg-Si) co-monomer, and subjected to gamma radiation, breaking down carried out for double bond of (AM), and (AN), the polymerization in the chain between (AM) and (AN) occurred by addition polymerization, where polymerization of (Mg-Si) in the chain was occurred by condensation polymerization [22-29], by elimination of OH^- of imine form with Na^+ of Na_2SiO_3 with formation of ionic bond between C atom of imine form and Si atom of

Na_2SiO_3 and elimination Na^+ from Na_2SiO_3 with Cl^- of $\text{MgCl}_2 \cdot 6\text{H}_2\text{O}$ with formation of ionic bond between O atom Na_2SiO_3 and Mg atom of $\text{MgCl}_2 \cdot 6\text{H}_2\text{O}$ and elimination of H^+ of solution with Cl^- of $\text{MgCl}_2 \cdot 6\text{H}_2\text{O}$ and lone pair of electron of N atom of (AN) were bonded by ionic bond with Mg atom of $\text{MgCl}_2 \cdot 6\text{H}_2\text{O}$ to form (AM-AN-Mg-Si) free radical. (AM-AN-Mg-Si) free radical reacts with (AM-AN-Mg-Si) co-monomer to form chain propagation. Finally, the chains were coupled with another (AM-AN-Mg-Si) free radical to obtain {P (AM-AN)-MgSi} composite.



SCHEME 4. Formation mechanism of polyacrylamide acrylic acid magnso-silicate composite



SCHEME 5. Formation mechanism of polyacrylamide acrylonitrile magnso-silicate composite.

The prepared samples of P (AM-AA), P (AM-AN), {P (AM-AA)-MgSi} and {P (AM-AN)-MgSi} composites are hard granulating in nature suitable for use in column operations with yellow color.

IR spectra of MgSi ion exchanger was shown in FIG. 1a, from this Figure six characteristic bands were observed in the regions 3150-3670, ~1652, 1000-1100, 903, 640 and ~ 470 cm^{-1} . The absorption band at 3150-3670 cm^{-1} may be attributed to the stretching mode of water and OH groups absorbed on the composite [1,22,23]. The strong band appear at ~1652 cm^{-1} represents the bending mode of water molecules absorbed on MgSi composite [1]. The broad absorption band at 1000-1100 cm^{-1} is due to the metal-oxygen (Mg-O) bond [1]. The band at $\approx 903 \text{ cm}^{-1}$ may be due to the Mg-OH deformation vibration or overlapping of the Si-O and Si-OH, and Mg-O bonds in the structure [1,24]. The broad bands at 640 and 470 cm^{-1} are assigned to Si-O-Mg and Si-O-Si bending vibrations, respectively [1,25].

IR spectra of P (AM-AA) copolymers prepared at radiation doses 25, 65 and 90 KGy was represented in FIG. 2a, from this Figure two bands observed at 3450 and 3354 cm^{-1} [26]. The first band may be attributed to the stretching mode of N-H bond of acrylamide and the second band attributed to the stretching mode of O-H of acrylic acid [27]. The band appeared at 3210 cm^{-1} cross ponding to the stretching mode of H-O-H bonded of water molecules [28,29]. The bands appeared at (3090, 2950 and 2870 cm^{-1}) may be due to the stretching mode of C-H of acrylamide and acrylic acid [30]. The strong band appeared at 1720 cm^{-1} attributed to the stretching mode of carbonyl group of acrylic acid [22,31]. Strong band appeared at 1550 cm^{-1} attributed to the bending mode of N-H bond of acrylamide [32]. Two bands appeared at 1450 and 1370 cm^{-1} may be attributed to the bending mode of C-H of acrylamide and acrylic acid [30,33]. Two broad bands appeared at 1213 and 1022 cm^{-1} attributed to the bending vibration of C-N of acrylamide [33,34].

IR spectra of P (AM-AN) copolymers prepared at radiation doses 25, 65 and 90 KGy was shown in FIG. 2b, from Figure represent, two bands appeared at 3340-3450 and 3195 cm^{-1} may be attributed to the stretching vibration of N-H bond of acrylamide [1,29]. Two bands observed at 2935 and 2875 cm^{-1} can be attributed to the stretching mode of C-H of acrylamide and acrylonitrile [35,36]. The band appeared at 2790 cm^{-1} may be due to the stretching mode of aldehyde group may be present by rearrangement in the structure [31]. The strong band appeared at 2244 cm^{-1} due to the stretching mode of $\text{C}\equiv\text{N}$ of acrylonitrile [35-38]. The band appeared at 1665 cm^{-1} attributed to the stretching mode of carbonyl group of acrylamide [32]. Band appeared at 1605 cm^{-1} may be attributed to the bending mode of N-H bond of acrylamide [32]. Two bands observed at 1450 and 1409 cm^{-1} may be attributed to the bending mode of C-H of acrylamide and acrylonitrile [34-37]. Three bands appeared at 1316, 1182 and 1120 cm^{-1} attributed to the bending vibration of C-N of acrylamide and acrylonitrile [32,34,37].

IR spectra of {P (AM-AA)-MgSi} composites prepared at radiation doses 25, 65 and 90 KGy was represented in FIG. 2c, this Figure show that; broad band observed at 3460-3200 cm^{-1} can be attributed to the stretching mode of water and OH group absorbed on the composites [1]. The two bands observed at 3460 and 3200 cm^{-1} can be

attributed to the stretching mode of N-H bond of acrylamide and H-O-H bonded of water molecules or O-H of acrylic acid respectively [27]. Two bands appeared at 2960 and 2875 cm^{-1} may be due to the stretching mode of C-H of acrylamide and acrylic acid [29-31]. Weak band appeared at 2245 cm^{-1} due to the stretching mode of $\text{C}\equiv\text{C}$ bond may be present by rearrangement in the structure [29,36]. Two bands appeared at 1725 and 1675 cm^{-1} , the former band may be due to the stretching mode of carbonyl group of acrylic acid [26,32], and the later band due to bending vibration of carbonyl group of acrylamide or due to presence of imine group or O-H bonded water molecules absorbed on the composite [32,39]. Band appeared at 1605 cm^{-1} for {P (AM-AA)-MgSi} at radiation dose 90 KGy attributed to the bending mode of O-H bonded water molecules absorbed on the composite [1]. The band appeared at 1571 cm^{-1} due to the bending mode of N-H bond of acrylamide [32]. Two bands appeared at 1451 and 1413 cm^{-1} may be attributed to the bending mode of C-H of acrylamide and acrylic acid [31,33,36]. Two bands appeared at 1331 and 1218 cm^{-1} for composite at radiation doses 25 and 65 KGy, where at 1331 and 1173 cm^{-1} for composite at radiation dose 90 KGy may be attributed to the bending mode of C-N of acrylamide [32]. Band appeared at 1104 cm^{-1} , this band reflect that metal oxygen bond Mg-O [1,17,18]. Three bands appeared at 793, 611 and 465 cm^{-1} . The first band may be attributed to the of Mg-OH deformation vibration or overlapping of the Si-O and Si-OH and Mg-O bonds in the structure [1,25]. The second band may be attributed to Si-O-Mg bending vibrations [25]. The third band may be due to Si-O-Si bending vibrations [1,25] the bands at 1104, 793, 611 and 465 cm^{-1} indicated that impregnation of Mg and Si in the polymeric resin, these results were agree with data obtained from XRF as will be set later.

IR spectra of {P (AM-AN)-MgSi} composites prepared at radiation doses 25, 65 and 90 KGy was shown in FIG. 2. (d), from this Figure broad band observed at 3475-3300 cm^{-1} can be attributed to the stretching mode of water and OH group absorbed on the composite or N-H bond of acrylamide [1,27]. Two bands observed at 3190 and 2940 cm^{-1} can be attributed to the stretching mode of N-H bond of acrylamide and C-H of acrylamide and acrylonitrile respectively, [34,36]. Strong band appeared at 2244 cm^{-1} due to the stretching mode of $\text{C}\equiv\text{N}$ bond of acrylonitrile [36]. Two bands appeared at 1661 and 1605 cm^{-1} , the first band may be attributed to the bending mode C=O group of acrylamide or due to presence of imine group [32], and the second band may be due to bending vibration of N-H bond of acrylamide or O-H bonded water molecules absorbed on the composite [1,36]. Two bands appeared at 1455 and 1413 cm^{-1} attributed to C-H of acrylamide and acrylonitrile [30]. Band appeared at 1571 cm^{-1} may be attributed to the bending mode of N-H bond of acrylamide [32]. Two bands appeared at 1451 and 1413 cm^{-1} may be attributed to the bending mode of C-H of acrylamide and acrylic acid [34-36]. Two bands appeared at 1340 and 1220 cm^{-1} for composite at radiation dose 25 KGy, where at 1340 and 1188 cm^{-1} for composite at radiation doses 65 and 90 KGy may be attributed to the bending mode of C-N of acrylamide [32]. The band appeared at 1040 cm^{-1} attributed to metal oxygen bond Mg-O [1,17,18]. Three bands appeared at 905, 636 and 460 cm^{-1} . The first band may be attributed to the of Mg-OH deformation vibration or overlapping of the Si-O and Si-OH and Mg-O bonds in the structure [1,25]. The second band may be attributed to Si-O-Mg bending vibrations [1,25]. The third band may be due to Si-O-Si bending vibrations [1,25]. The bands at 1040, 905, 636 and 460 cm^{-1} indicated that impregnation of

Mg and Si in the structure of polymeric resin, these results were agree with data obtained from XRF as will be set later.

X-ray diffraction patterns of MgSi composite were represented in FIG.1b, from this Figure it is clear that Mg-Si has crystalline structure [1,40]. These results were agree with the data obtained from XRD of composites materials treated at different heating temperature [1,11,14]. The crystallinity of the prepared materials slightly improved with the increase of heating temperatures from 50°C to 850 ± 1°C, and there is a sharp improvement of crystallinity occurs at 850 ± 1°C.

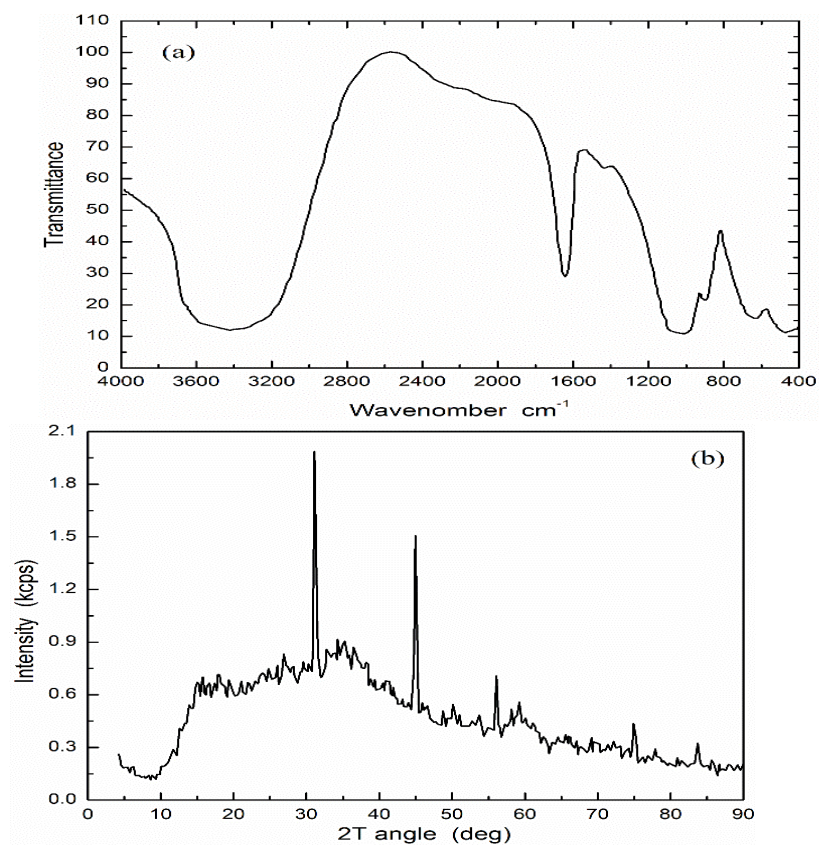


FIG.1. (a) IR spectrum of magnesio-silicate; (b) XRD of magnesio-silicate.

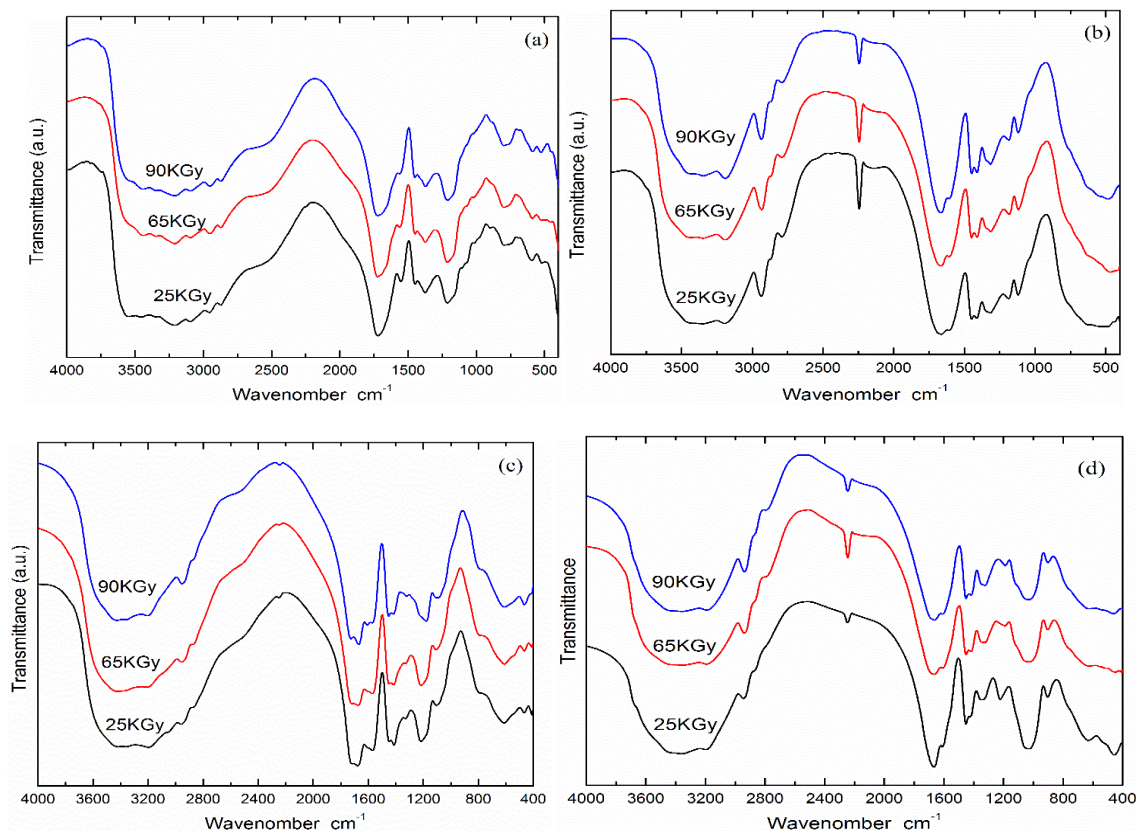


FIG.2. (a) IR spectrum of P (AM-AA); (b) P (AM-AN); (c) {P (AM-AA)-MgSi}; (d) {P (AM-AN)-MgSi} at different radiation doses.

FIG.3a shows that XRD of P (AM-AA) copolymers prepared at radiation doses 25, 65 and 90 KGy. This Figure indicated that P (AM-AA) copolymers have amorphous structure and these results were similar to the data obtained from XRD of polyacrylamide-co-acrylic acid prepared by Hassan, et al. [31]. In addition, the crystalline character of the prepared samples was increased with radiation doses from 25 to 90 KGy. FIG. 3b shows XRD patterns for P (AM-AN) copolymers prepared at radiation doses 25, 65 and 90KGy. From this figure it is clear that the sample prepared at radiation dose 25 KGy has crystalline structure, and these results were similar to the data obtained from XRD of potassium hexacyano cobalt (II) ferrate (II) polyacrylonitrile (KCFC-PAN) [41], where samples prepared at radiation doses 65 and 90 KGy have amorphous structure.

FIG. 3c and 3d show XRD patterns of {P (AM-AA)-MgSi} and {P (AM-AN)-MgSi} composites prepared at radiation doses 25, 65 and 90 KGy, respectively. From these figures it is clear that P (AM-AA)-MgSi and P (AM-AN)-MgSi have crystalline structure and these results were similar to the data obtained from XRD of polyacrylamide titanium tungstophosphate [19,42], and potassium hexacyano cobalt (II) ferrate (II) polyacrylonitrile

(KCFC–PAN) [41]. In addition, the crystalline character of {P (AM-AA)-MgSi} samples were decreased with radiation dose from 25 to 90 KGy, where the samples prepared at radiation doses 25 and 65 KGy have crystalline nature, where sample prepared radiation dose 90KGy have semi crystalline nature. On the other hand, the crystalline character {P (AM-AN)-MgSi} was decreased with radiation doses from 25 to 65 KGy then increase from 65 to 90 KGy, where the sample at radiation dose 65 and 90 KGy has amorphous and semi crystalline natures, respectively.

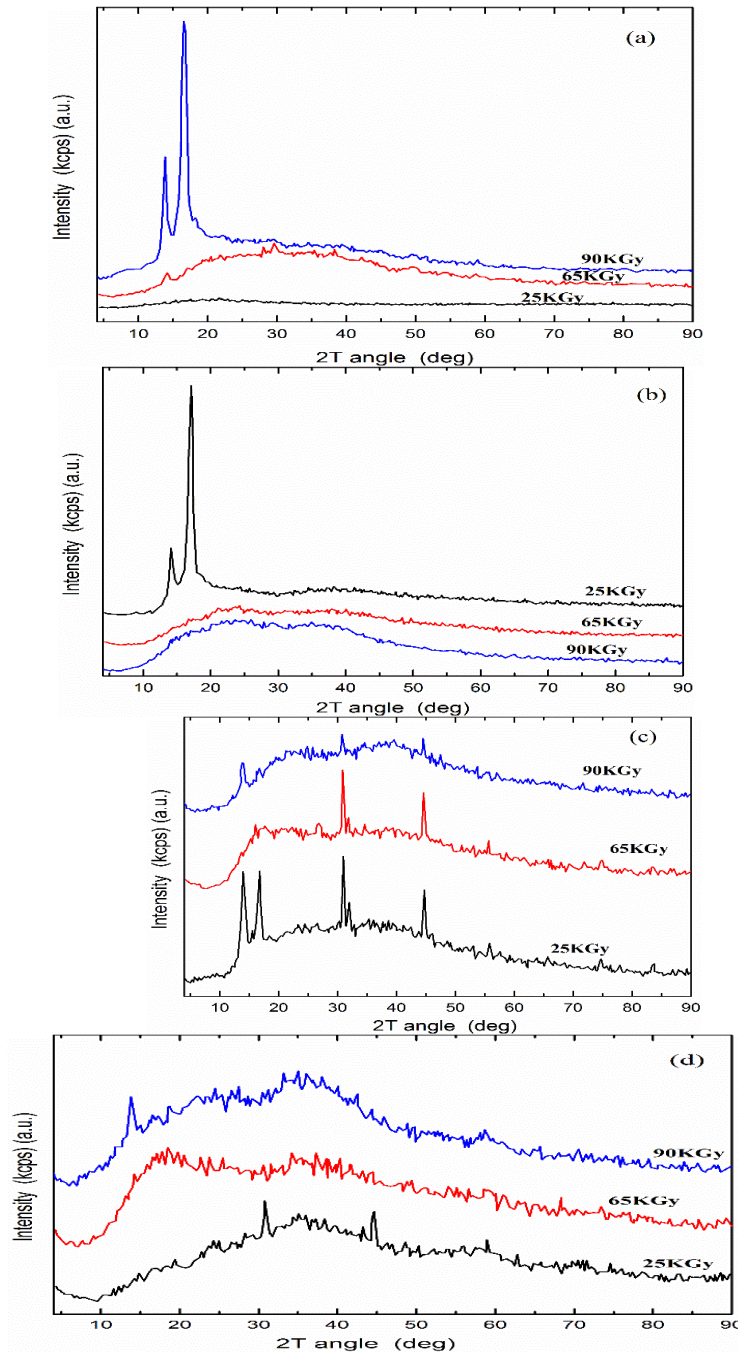


FIG.3. (a) XRD of P (AM-AA); (b) P (AM-AN); (c) {P (AM-AA)-MgSi}; (d) {P (AM-AN)-MgSi} at different radiation doses.

Differential thermal and thermogravimetric analyses (DTA&TGA) play a vital role in studying the structure and the properties of any materials where it has been widely used to investigate the decomposition characteristics of materials. DTA and TGA data were used here to provide an alternative model for the kinetics of the composite degradation. For all investigation studies of the composites the rate of heating is 10°C/min [17,34,42,43], and the data were tabulated in TABLES 1 and 2.

TABLE 1. DTA and TGA analyses for MgSi, P (AM-AA) and P (AM-AN) materials.

Temp., °C	Temp. Range, °C	Peak	Peak Description	Ref.
28.35	43-192	Endo.	Crossbedding loss of free water	1,47
57.2	192-283	Exo.	Due to decomposition of residual OH-groups and condensation of non-bonded oxygen	48
101.16	283-800	Endo.	The loss of chemical bond water	1,47
19.29	44-125	Endo.	Loss of external water molecule	49
19.88	125-240	Endo.	Removal of the water of crystallization for P (AM-AA)	50
38.27	240-384	Endo.	Probably caused by the dehydration of carboxylic acid and decarboxylation or the loss of chemical bond water	1,47,51
100.9	384-408	Exo.	May be due to the complete decomposition of the organic part of the materials	52-54
22.28	408-500	Endo.	The chain scission in the main chain of poly acrylamide acrylic acid.	51
86.6	40-137	Endo.	Loss of external water molecule	49
219	137-253	Endo.	Removal of the water of crystallization for P (AM-AA)	50
30.7	253-352	Endo.	Probably caused by the dehydration of carboxylic acid and decarboxylation or the loss of chemical bond water	1,47,51
62.47	352-378	Exo.	may be due to the complete decomposition of the organic part of the materials	52-54
92.56	378-500	Endo.	The chain scission in the main chain of poly acrylamide acrylic acid.	51
11.69	41-129	Endo.	Loss of external water in the resin	49
22.45	129-248	Endo.	Removal of the water of crystallization for P (AM-AA)	50
74.7	248-311	Exo.	Since the complete decomposition of the organic part of the materials	52-54
20.9	311-347	Endo.	Due to dehydration of carboxylic acid and decarboxylation or the loss of chemical bond water	1,47,51
50.08	347-367	Exo.	the complete decomposition of the organic part of the materials	52-54
86.55	367-398	Endo.	The loss of constitution water, which forms part of the crystalline network and it is generally presented like OH groups	55-56
20.34	398-427	Exo.	may be due to the complete decomposition of the organic part of the composites	52-54
76.5	427-500	Endo.	The chain scission in the main chain of poly acrylamide acrylic acid.	51
0.5	54-133	Endo.	loss of external water present in the composite	49
73.1	133-328	Endo.	Due to removal of the water of crystallization for P (AM-AN) copolymer	50
72.4	328-384	Exo.	Due to the complete decomposition of the organic part of the materials	52-54

93.5	384-418	Endo.	The loss of constitution water, which forms part of the crystalline network and it is generally presented like OH groups	55, 56
36.4	418-452	Endo.	The chain scission in the main chain of poly acrylamide acrylic acid	51
65.7	452-500	Endo.		
3.43	50-145	Endo.	Loss of external water molecule	49
73.3	178-312	Endo.	Removal of the water of crystallization for P (AM-AN)	50
62.8	312-367	Exo.	Due to the complete decomposition of the organic part of the polymer	52-54
78.2	367-400	Endo.	The loss of constitution water, which forms part of the crystalline network and it is generally presented like OH groups	55, 56
69.7	400-500	Endo.	The chain scission in the main chain of poly acrylamide acrylic acid.	51
5.63	57-137	Endo.	loss of external water molecule	49
40.4	137-286	Endo.	removal of the water of crystallization for P (AM-AN)	50
57.4	286-416	Endo.	The loss of constitution water, which forms part of the crystalline network and it is generally presented such as OH groups	55, 56
37.8	416-456	Exo.	Due to the complete decomposition of the organic part of the resin	52-54
69.5	456-500	Endo.	The chain scission in the main chain of poly acrylamide acrylic acid.	51

TABLE 1 was represented the data obtained for DTA and TGA analyses for inorganic ion exchange material MgSi and organic polymers P (AM-AA) and P (AM-AN) radiated at different radiation doses 25, 65 and 90 KGy. The data obtained are supporting the fact that MgSi have a good thermal stability comparing with the other inorganic ion exchangers and the weight loss of MgSi when the sample calcinated at 800 °C equal to 33.4% [1].

DTA and TGA of P (AM-AA) and P (AM-AN) copolymers prepared at radiation doses 25, 65 and 90 KGy were represented in TABLE 1 and indicates the process was occurring via five stage process and the weight loss are continued up to 500°C. The weight loss for P (AM-AA) and P (AM-AN) prepared at radiation doses 25, 65 and 90 KGy with the heating temperature indicates that a (67.15%, 100% and 68.3%) for P (AM-AA) and (56.98%, 61.3% and 25.5%) for P (AM-AN) when the samples are calcinated at 500°C [19] (TABLE 3).

TABLE 2. DTA and TGA analyses for {P (AM-AA)-MgSi} and {P (AM-AN)-MgSi} composite materials.

Temp., °C	Temp. Range, °C	Peak	Peak Description	Ref.
0.92	38-139	Endo.	Caused by loss of external water molecule	49
63.7 2	139-313	Endo.	Removal of the crystalline water for {P (AM-AA)-MgSi}	50
96.1 4	340-434	Exo.	The complete decomposition of the organic part of the composite.	52-54
34.1	434-517	Endo.	Probably caused by the dehydration of carboxylic acid and decarboxylation or the loss of chemical bond	1,47,49,51

8			water	
55.6	517-800	Endo.	The chain scission in the main chain of poly acrylamide acrylic acid.	51
2.17	67-164	Endo.	Loss of external water molecule	49
04.5	164-355	Endo.	Removal of the chemical bond water of {P (AM-AA)-MgSi}	50
75.1 5	355-409	Exo.	The complete decomposition of the organic part of the composite resin	52-54
29.1 9	409-455	Exo.		
21.1 9	455-563	Exo.		
30.8	42-171	Endo.	Loss of free water molecule	49
40.1 6	171-318	Endo.	Removal of the crystalline water for {P (AM-AA)-MgSi}	50
80.3 3	318-407	Exo.	The complete decomposition of the organic part of the composite ion exchangers	52-54
20.5 5	407-431	Endo.	Due to loss of chemical bond water	1,47
44.0 5	431-467	Exo.	May be due to the complete decomposition of the organic part of the materials	52-54
03.7 8	467-800	Exo.		
6.26	57-132	Endo.	Loss of water molecule	49
81.6 9	132-340	Endo.	Removal of the water of crystallization for {P (AM-AN)-MgSi}	50
72.1 3	340-398	Exo.	The complete decomposition of the organic part of the composites	52-54
19.6 9	398-433	Endo.	The loss of interstitial water molecules	1,47
15.5 8	434-577	Exo.	May be due to the complete decomposition of the organic part of the materials	52-54
85.5 6	577-800	Endo.	The chain scission in the main chain of poly acrylamide acrylic acid.	51
6.24	40-124	Endo.	Loss of free water molecule	49
63.5 1	124-334	Endo.	Removal of the water bind molecules of {P (AM-AN)-MgSi}	50
62.7 2	334-383	Exo.	The complete decomposition of the organic part of the ion exchange materials	52-54
98.5 7	383-402	Endo.	The loss of chemical bond water	1,47
48.3 8	402-472	Exo.	May be due to the complete decomposition of the organic part of the materials	52-54
21.2 9	472-800	Exo.		
6.11	55-126	Endo.	Loss of non-bonded water molecule	49
72.6 3	126-326	Endo.	Removal of the water of crystallization for {P (AM-AN)-MgSi}	50
65.2	326-397	Exo.	may be due to the complete decomposition of the organic part of the materials	52-54
21.2 9	397-452	Endo.	The loss of chemical bond water	1,47
27.2	452-800	Exo.	The complete decomposition of the organic part of the composite materials	52-54

TABLE 3. Elemental analysis of magnesio-silicate and polymeric composites based on silicate prepared at different radiation doses

Composite	Radiation Dose, KGy	Concentration, %	
		Mg	Si
MgSi	----	18.7	37.7
P (AM-AA)-MgSi	25	10.1	21.2
	65	11.6	25.6
	90	8.3	44.7
P (AM-AN)-MgSi	25	13.3	44.7
	65	12.9	47.6
	90	13.5	45.2

The DTA and TGA analyses for polymeric materials impregnated with inorganic ion exchange materials, {P (AM-AA)-MgSi} and {P (AM-AN)-MgSi} prepared at different radiation doses 25, 65 and 90 KGy were measured and tabulated in TABLE 2. The data in TABLE 2 indicates that the process for {P (AM-AA)-MgSi} composite was occurring via four stage process at radiation doses 25 and 90 KGy, where five stage process at radiation doses 65 KGy. On the other hand, the process for {P (AM-AN)-MgSi} prepared at radiation doses 25, 65 and 90 KGy occurs via four stage process. Also, the data supporting the fact that {P (AM-AA)-MgSi} composites prepared at radiation doses 25, 65 and 90KGy have a good thermal stability comparing with the other inorganic ion exchangers. The weight losses of {P (AM-AA)-MgSi} composites prepared at radiation doses 25, 65 and 90 KGy with the heating temperature equal 100%, 88.34% and 88.8% when the samples are calcinated at 800 °C. also, TABLE 2 indices that, the weight loss for {P (AM-AN)-MgSi} prepared at radiation doses 25, 65 and 90KGy are continued up to 600°C, and no weight loss occurred in the range ~600-800°C. This supporting the fact that {P (AM-AN)-MgSi} prepared at radiation doses 25, 65 and 90KGy have a good thermal stability comparing with the other inorganic ion exchangers. The weight losses of {P (AM-AN)-MgSi} prepared at radiation doses 25, 65 and 90 KGy with the heating temperature equal to 74.2%, 80.8% and 83.9% when the sample is calcinated at 800°C [1,19].

The elemental analyses of magnesio-silicate and polymeric composites based on silicate prepared at different radiation doses were measured using XRF and tabulated in TABLE 3; the measured data is confirmed that impregnation of magnesio-silicate in the {P (AM-AA)-MgSi} and {P (AM-AN)-MgSi} [44,45].

Conclusion

Magnesio-silicate (MgSi) has been synthesized by precipitation technique. P (AM-AA), P (AM-AN), {P (AM-AA)-MgSi} and {P (AM-AN)-MgSi} composites have been synthesized by subjected co-monomers to gamma radiation initiated polymerization at radiation doses 25, 65 and 90 KGy. From the data obtained from the analytical techniques such as IR, XRD, TGA, DTA and XRF it is indicating that the impregnation of MgSi in {P (AM-AA)-MgSi} and {P (AM-AN)-MgSi} show an improvement in thermal stability and these composite materials have crystalline nature suitable for column chromatographic applications [46-57].

REFERENCES

1. Abou-Mesalam MM, Abass MR, Abdel-Wahab MA, et al. Complex doping of d- block elements cobalt, nickel and cadmium in magnesio- silicate composite and its use in the treatment of aqueous waste, desalination and water treatment. 2016:1–8.
2. Abou-Mesalam MM. Application of inorganic ion exchangers; II-adsorption of some heavy metal ions from their aqueous waste solution using synthetic iron (III) titanate, *J. of Adsorption*. 2004;10:87-92.
3. Vetrivel V, Santhi RJ. Synthesis and characterization of poly acrylic acid modified with dihydroxy benzene-redox polymer. *Res. J. Chem. Sci.* 2014;4 (5):1-9.
4. Hoogenboom R, Poly (2-oxazoline): Alive and kicking, *Macromol. Chem. Phys.* 2007;208:18-25.
5. Angiolini L, Benelli T, Giorgini L, et al. Synthesis of optically active methacrylic oligomeric models and polymers bearing the side-chain azo-aromatic moiety and dependence of their chiroptical properties on the polymerization degree. *Polym.* 2006;47:1875–885.
6. Rosseinsky DR, Mortimer R. Electrochromic systems and the prospects for devices. *J Adv Mater.* 2001;13:783-93.
7. Grote JG, Zetts JS, Nelson RL, et al. Effect of conductivity and dielectric constant on the modulation voltage for optoelectronic devices based on nonlinear optical polymers. *Opt. Eng.* 2001;40:2464-473.
8. Eugenio K, Itamar W. A biofuel cell with electrochemically switchable and tunable power output. *J. Am. Chem. Soc.* 2003;125:6803-813.
9. Luqman M. Ion exchange technology I theory and materials. King Saud University, Kingdom of Saudi Arabia. 2012.
10. Abou-Mesalam MM, Hilal MA, Arida HA, Environmental studies on the use of synthesized and natural ion exchange materials in the treatment of drinking and underground water. *Arab J. of Nuc. Sci. and App.* 2013;46 (3):63-74.
11. Abou-Mesalam MM, El-Naggar IM. Selectivity modification by ion memory of magnesio-silicate and magnesium alumino-silicate as inorganic sorbents. *J. of Haz. Mat.* 2008;154:168–74.
12. Gando-Ferreira LM. Ion exchange technology II: Application. Springer Science and Business Media B.V. 2012.
13. Lee YK, Jeong JM, Hoigebazar L, et al. Nanoparticles modified by encapsulation of ligands with a long alkyl chain to affect multispecific and multimodal imaging. *J. of nuclear medicine.* 2012;53 (9).
14. El-Naggar IM, Abou-Mesalam MM. Novel inorganic ion exchange materials based on silicates; synthesis, structure and analytical applications of magnesio-silicate and magnesium alumino-silicate sorbents. *J. of Haz. Mat.* 2007;149:686–92.
15. Clowutimon W, Kitchaya P, Asswasaengrat P. Adsorption of free fatty acid from crude palm oil magnesium silicate derived from rice husk. *Engineering J.* 2011;15 (3).

16. Abou-Mesalam MM, Amine AS, Abdel-Aziz MM, et al. Synthesis and ion exchange characteristic of poly (acrylamide-acrylic acid)-silicon titanate and its use for treatment of industrial waste. *J. Chem.* 2000;46 (5):655-70.
17. Borai EH, Hamed MG, El-kamash AM, et al. Synthesis, characterization and application of a modified acrylamide–styrene sulfonate resin and a composite for sorption of some rare earth elements. *New Journal of Chemistry*, 2015;39:7409-420.
18. Abou-Mesalam MM, El-Naggar IM. Chromatographic separations of traces ^{134}Cs , ^{60}Co , and $^{152,154}\text{Eu}$ using silico-, molybdo-, and chromo-titanates as inorganic ion exchangers. *Industrial & Engineering Chemistry Research*. 2008;47 (17):6753-758.
19. El-Zahhar AA, Abdel-Aziz HM, Siyam T. Gamma radiation-induced preparation of polymeric composite sorbents and their structure assignments. *J. of Macromolecular Science Part A Pure and Applied Chemistry*. 2007;44 (2):215222.
20. Siyam T. The chemistry and properties of poly (acrylamide-acrylic acid) resins. *J. of Macromolecular Science Part A*. 1999;36 (3):405-15.
21. Odian G. *Principles of Polymerization*, 4th ed., John Wiley, New York. 2004.
22. El-Naggar IM, Mowafy EA, Al-Aryan YF, et al. Sorption mechanism for Cs^+ , Co^{2+} and Eu^{3+} on amorphous zirconium silicate as cation exchanger. *Solid State Ionics*. 2007;178 (11):741-47.
23. Zhang H, Simpson D, Kumar S, et al. Interaction of hydroxylated PACVD silica coatings on titanium with simulated body fluid. *Colloids and Surfaces A: Physicochemical and Engineering Aspects*. 2006;291:128-38.
24. Al-Degs YS, El-Barghouthi MI, Issa AA, et al. Sorption of Zn (II), Pb (II), and Co (II) using natural sorbents: Equilibrium and kinetic studies, *Water Research*, 2006;40:2645-658.
25. Madejova J, FTIR techniques in clay mineral studies. *Vib. Spectrosc.* 2003;31:1-10.
26. D Li, M Wang, C Yang, et al. Solid state characterizations and analysis of stability in azelnidipine polymorphs. *Chemical & Pharmaceutical Bulletin*. 2012;60 (8):995-002.
27. N Al-Yassir, R Le Van Mao. Catalysts for the thermo-catalytic cracking (TCC) process: Interactions between the yttria in yttria-doped alumina aerogel and the mono-oxide MoO_3 , CeO_2 , and bi-oxide $\text{MoO}_3\text{-CeO}_2$ species. *Applied Catalysis A, General*. 2007;332:273-88.
28. B Semagne, I Diaz, T Kebede. Synthesis, characterization and analytical application of polyaniline tin (IV) molybdophosphate composite with nanocrystalline domains. *Reactive and Functional Polymers*. 2016;98:17-23.
29. SA Nabi, SA Ganai, AM Khan. Synthesis, characterization and ion exchange behavior of polyaniline stannic silicomolybdate, an organic–inorganic composite material: Quantitative separation of Pb^{2+} ions from industrial effluents. *J. IOP*. 2011;21 (1):25-35.
30. Silverstein RM, Webster FX, Kiemle D. *Spectrometric identification of organic compounds*. John Wiley, New York, USA; 2005.

31. Hassan MF, Yusof SZM. Poly (Acrylamide-Co-Acrylic Acid)-zinc acetate polymer electrolytes: Studies based on structural and morphology and electrical spectroscopy. *Microscopy Research*. 2014;2:30-38.
32. Dawood AS, Yilian L. Wastewater flocculation using a new hybrid copolymer: Modeling and optimization by response surface methodology, *Pol. J. Environ. Stud*. 2014;23 (1):43-50.
33. Abdel-Galil EA, Rizk HE, Mostafa AZ. Production and characterization of activated carbon from *Leucaena* plant wastes for removal of some toxic metal ions from waste solutions. *Desalination and Water Treatment*. 2015;57 (38):17880-7891.
34. Wang Q, Dong Z, Du Y, et al. Controlled release of ciprofloxacin hydrochloride from chitosan/polyethylene glycol blend films. *Carbohydr Polym*. 2007;69 (2):336-43.
35. Barron C, Rouau X. FTIR and Raman signatures of wheat grain peripheral tissues. *Cereal Chemistry*. 2008;85 (5):619-25.
36. Lee S, Kim J, Ku BC, et al. Structural evolution of polyacrylonitrile fibers in stabilization and carbonization. *J. Adv. in Chem. Eng. and Sci*. 2012;2:275-82.
37. Saufi SM, Ismail AF. Development and characterization of polyacrylonitrile (PAN) based carbon hollow fiber membrane. *J. Sci. Technol*. 2002;24:843-54.
38. Bhuvanewari MS, Selvasekarapandian S, Kamishima O, et al. Vibrational analysis of lithium nickel vanadate. *Journal of Power Sources*. 2005;139 (1-2):279-83.
39. Fujimoto A, Lwasaki N, Hikiba Y, et al. Raman spectroscopic study of 1- methyl-2 (1H)-pyridinimine, the deuterated analog, and 1-methyl-2 (1H)-pyridinone. *Spectrochimica Acta Part A: Molecular and Biomolecular Spectroscopy*. 1998;54 (12):1779-792.
40. JCPDS- Joint Committee on Powder Diffraction Standards, International center for diffraction data, 1997.
41. Nilchi A, Khanchi A, Atashi H, et al. The application and properties of composite sorbents of inorganic ion exchangers and poly acrylonitrile binding matrix. *Journal of Hazardous Materials*. 2006;137:1271-276.
42. Abdel-Galil EA, Sharaf El-Deen GE, El-Aryan YF, et al. Preparation of hybrid ion exchanger based on acrylamide for sorption of some toxic metal ions from aqueous waste solutions, *Russ. J. Appl. Chem*. 2016;89 (3):467-79.
43. Hashem A, Abdel-Halim ES, Sokker HH. Bi-functional starch composites prepared by γ -irradiation for removal of anionic and cationic dyes from aqueous solutions. *Polymer-Plastics Technology and Engineering*. 2007;46 (1):71-77.
44. Lihong F, Yang J, Wu H, et al. Preparation and characterization of quaternary ammonium chitosan hydrogel with significant antibacterial activity. *Int. J. Biol. Macromol*. 2015;79:830-36.
45. Attallah MF, Borai EH, Hilal MA, et al. Utilization of different crown ethers impregnated polymeric resin for treatment of low level liquid radioactive waste by column chromatography. *J Hazard Mater*. 2011;195:73-81.
46. Allan KF, El Afifi EM, Holial M. Synthesis and application of poly (Acrylamide-Itaconic Acid)/zirconium tungstate composite material for cesium removal from different solutions. *Particulate Science And Technology*. 2015:1-12.

47. Hamoud MA, Allan KF, Sanad WA, et al. Gamma irradiation induced preparation of poly (acrylamide–itaconic acid)/zirconium hydrous oxide for removal of Cs-134 radionuclide and methylene blue. *J. Radioanal Nucl Chem.* 2014;302:169-78.
48. Abou-Mesalam MM. Sorption kinetics of copper, zinc, cadmium and nickel ions on synthesized silico-antimonate ion exchanger. *J. Colloids and Surfaces. A: Physicochem. Eng. Aspects.* 2003;225:85.
49. Duval C. *Inorganic thermogravimetric analysis.* Amsterdam: Elsevier. 1963:315.
50. Ali IM, Kotp YH, El-Naggar IM. Thermal stability, structure modifications and ion exchange properties of magnesium silicate, *Desal.* 2010;259:228-34.
51. Trong-Ming D, Chung-Yang C, Wen-Yen C. Tamkang, studies on the degradation behavior of chitosan-g-poly (acrylic acid) copolymer. *J. of Science and Engineering.* 2002;5 (4):235-40.
52. Khan AA, Alam MM, Mohamed I. Electrical conductivity and ion exchange kinetic studies of a crystalline type 'organic-inorganic' cation-exchange material: Polypyrrole/polyantimonic acid composite system, (Sb₂O₅) (-C₄H₂NH-).nH₂O, *J. Electroanal. Chem.* 2004;572 (1):67-78.
53. Lanthong P, Nuisin R, Kiatkamjornwong S, et al. Graft copolymerization, characterization, and degradation of cassava starch-g acrylamide/itaconic acid super absorbents, *Carbohydr Polym.* 2006;66:229–45.
54. El-Aryan YF, Abdel-Galil EA, Sharaf GE, et al. Synthesis, characterization, and adsorption behavior of cesium, cobalt, and europium on polyacrylonitrile titanium tungstophosphate organic–Inorganic hybrid exchanger. *Russ. J. Appl. Chem.* 2015;88 (2):516-23.
55. El-Naggar IM, Hebash KA, Sheneshen ES, et al. Preparation, characterization and ion exchange properties of a new 'organic-inorganic' composite cation exchanger poly aniline silicotitanate: its applications for treatment of hazardous metal ions from waste solutions. *Inorganic chemistry.* 2014;9 (1):1-14.
56. Ali IM, Gomaa MA, El-Naggar, et al. Sorption performance of lithium-doped titanium vanadate for Sr²⁺, Fe³⁺ and Al³⁺ from polluted water. *Desalination and Water Treatment.* 2015;57 (31):14552-4564.
57. Nabi SA, Bushra R, Al-Othman ZA, et al. Synthesis, characterization, and analytical applications of a new composite cation exchange material acetonitrile stannic (IV) selenite: Adsorption behavior of toxic metal ions in nonionic surfactant medium. *Separation Science and Technology.* 2011;46 (5):847-57.